

# Bilayer Interactions of pHLIP, a Peptide that Can Deliver Drugs and Target Tumors

Manuela Zoonens,\* Yana K. Reshetnyak,<sup>†</sup> and Donald M. Engelman\*

\*Department of Molecular Biophysics and Biochemistry, Yale University, New Haven, Connecticut; and <sup>†</sup>Physics Department, University of Rhode Island, Kingston, Rhode Island

**ABSTRACT** The pH-dependent insertion of pHLIP across membranes is proving to be a useful property for targeting acidic tissues or tumors and delivering drugs attached to its C-terminus. It also serves as a model peptide for studies of protein insertion into membranes, so further elucidation of the insertion mechanism of pHLIP and its features is desirable. We examine how the peptide perturbs a model phosphatidylcholine membrane and how it associates with the lipid bilayer using an array of fluorescence techniques, including fluorescence anisotropy measurements of TMA-DPH anchored in bilayers, quenching of pHLIP fluorescence by brominated lipids and acrylamide, and measurements of energy transfer between aromatic residues of pHLIP and TMA-DPH. When pHLIP is bound to the surface of bilayers near neutral pH, the membrane integrity is preserved whereas the elastic properties of bilayers are changed as reported by an increase of membrane viscosity. When it is inserted, there is little perturbation of the lipids. The results also suggest that pHLIP can bind to the membrane surface in a shallow or a deep mode depending on the phase state of the lipids. Using parallax analysis, the change of the penetration depth of pHLIP was estimated to be 0.4 Å from the bilayer center and 2.8 Å from the membrane surface after the liquid-to-gel phase transition.

## INTRODUCTION

The isolated C-helix of bacteriorhodopsin has been observed previously to be water-soluble, to bind to lipid bilayer surfaces as an unstructured peptide above pH 7, and to spontaneously insert as an  $\alpha$ -helix across lipid bilayers in a pH-dependent manner, with a  $pK_{app}$  of 6 (1). The insertion of this peptide, dubbed pHLIP, for pH low insertion peptide, is reversible and oriented such as the C-terminus is translocated across the membrane whereas the N-terminus stays outside of the membrane (2,3). The insertion mechanism is coupled to the protonation of one or both of two aspartic acid residues located in the transmembrane part of the peptide (Asps at positions 85 and 96 in the bacteriorhodopsin sequence) (1,4). The thermodynamics of pHLIP binding and insertion in membranes has been analyzed in detail (1,5), and its three major forms (soluble in aqueous solution, bound at the membrane surface, and inserted across a lipid bilayer) were

found to be monomeric at peptide concentrations less than  $\sim 7 \mu\text{M}$  (3).

Owing to its exceptional characteristics, pHLIP can be used as a model peptide for studying membrane protein folding and insertion in lipid bilayers, or as a tool for therapeutic drug delivery. Individual peptides that mimic transmembrane sections of membrane proteins are suitable model systems for biophysical studies to obtain an insight into the molecular interactions that play a role in the native system (6–8). Such an approach is rationalized by the two-stage process model of membrane protein folding, when individual helices first insert and, then, oligomerize to form higher order structures (9,10). Folding pathways for membrane proteins can be based on this model even if additional steps are often required for achieving the final equilibration of native and functional structures in vivo (11). Studying a single helix may thus provide an insight into the folding of more complex membrane proteins (12,13).

Biological membranes are the main barriers for therapeutic drug delivery. The energy released as a result of pHLIP insertion into a membrane can be used to move cell-impermeable cargo molecules across a membrane into a cell (2). The ability of pHLIP to target cells in an extracellular acidic environment, which is associated with tumors and other pathological conditions, has been confirmed in vivo by whole-body fluorescence and positron emission tomography imaging (4,14). pHLIP has also been shown to induce shape changes of RBCs at neutral pH, consistent with the idea that peptide binding perturbs the bilayer structure, whereas at low pH, i.e., when the peptide is inserted in lipid bilayers, the perturbations are absent (4).

The objective of this study is to gain further insights into the interaction of pHLIP with a lipid bilayer both for fun-

Submitted October 19, 2007, and accepted for publication February 28, 2008.

Address reprint requests to Manuela Zoonens, Tel.: 33 1 40 61 56 97; Fax: 33 1 40 61 56 73; E-mail: [mzoonens@necker.fr](mailto:mzoonens@necker.fr).

Manuela Zoonens' present address is UPR 9078, CNRS, Faculté de Médecine René Descartes Paris 5, Site Necker-Enfants Malades, 156 rue de Vaugirard, 75730 Paris Cedex 15, France.

**Abbreviations used:** (6-7)Br<sub>2</sub>-PC, 1-palmitoyl-2-stearoyl(6-7)dibromo-*sn*-glycero-3-phosphocholine; (9-10)Br<sub>2</sub>-PC, 1-palmitoyl-2-stearoyl(9-10)dibromo-*sn*-glycero-3-phosphocholine; CD, circular dichroism; DMPC, 1,2-dimyristoyl-*sn*-glycero-3-phosphocholine; DPPC, 1,2-dipalmitoyl-*sn*-glycero-3-phosphocholine; FRET, Förster resonance energy transfer; LUV, large unilamellar vesicle; Mops, 4-morpholinepropanesulfonic acid; pHLIP, pH low insertion peptide; POPC, 1-palmitoyl-2-oleoyl-*sn*-glycero-3-phosphocholine; RBC, red blood cell;  $T_m$ , melting temperature of the lipid phase transition; TMA-DPH, 1-(4-trimethylammoniumphenyl)-6-phenyl-1,3,5-hexatriene *p*-toluenesulfonate.

Editor: Thomas J. McIntosh.

© 2008 by the Biophysical Society  
0006-3495/08/07/225/11 \$2.00

doi: 10.1529/biophysj.107.124156

damental understanding and to facilitate the rational design of sequences that insert into cell membranes in a controlled way. The strain that pHLIP induces in a bilayer when it is bound to its surface, the positioning of the peptide at the bilayer surface in the liquid-crystal and gel phases, and the changes on membrane insertion were investigated in detail by a variety of biophysical methods.

## MATERIALS AND METHODS

### Materials

Mops was purchased from Roche Diagnostics (Indianapolis, IN). Urea, melittin peptide from honey bee venom, and Triton X-100 were supplied by Sigma-Aldrich (St. Louis, MO). One M Tris-HCl pH 8 solution was from American Bioanalytical (Natick, MA). The pH of the samples was checked using a MI-415 pH combination electrode supplied by Microelectrodes (Bedford, MA). POPC, DMPC, DPPC, (6-7)Br<sub>2</sub>-PC, and (9-10)Br<sub>2</sub>-PC in chloroform, and a mini-extruder were purchased from Avanti Polar Lipids (Alabaster, AL). TMA-DPH and calcein were from Invitrogen Molecular Probes (Carlsbad, CA). The HiPrep 26/10 Desalting column and the Äkta FPLC system were from GE Healthcare Life Sciences (Piscataway, NJ). Slide-A-lyser dialysis cassettes of 3,500 Da cutoff (0.5 to 3 mL capacity) were from Pierce Biotechnology (Rockford, IL). pHLIP with the following sequence GGEQNPIYWARYADWLFTPLLLDLALLVDADEGT and the variant with the six last residues in C-terminus, -NANQGT were chemically synthesized and purified (>95%) by Biopeptide (San Diego, CA).

### Preparation of pHLIP sample

A lyophilized powder of the peptide was dissolved at 1 mg mL<sup>-1</sup> in 8 M urea, 20 mM Tris-HCl, 50 mM NaCl, pH 8. After vortexing, the sample was dialyzed four times against 500 mL of the same buffer without urea. The buffer was exchanged for 20 mM Mops, 50 mM NaCl, pH 7.9 over four additional dialysis baths. The final concentration of pHLIP was determined by UV absorption using a molar extinction coefficient of  $\epsilon_{280} = 13,940 \text{ M}^{-1} \text{ cm}^{-1}$  (2).

### Preparation of vesicle suspensions

Five milligrams of lipids in chloroform (the initial concentrations were 25 mg mL<sup>-1</sup> for POPC and 10 mg mL<sup>-1</sup> for DMPC) were dried in a rotary evaporator and then held under vacuum overnight. The dried lipid film was rehydrated with 1 mL of water and vortexed. The resulting vesicles were subjected to five cycles of freeze-thawing to produce liposomes, which then were extruded (25 times using a mini-extruder) through 100 nm pore diameter filters to obtain LUVs. Lipid concentration was checked using Marshall's assay (15).

### Steady-state anisotropy measurements

LUVs were prepared from DMPC according to the protocol described above and TMA-DPH in methanol was added from a 5 mM stock solution to give a final probe/lipid molar ratio of 1:500 (0.2 mol %). To allow the probe to be incorporated, liposomes were incubated at 30°C (i.e., above  $T_m$ ) for at least 1 h before use. Increasing concentrations of pHLIP peptide (0.2, 0.4, 1.0, and 2.0 mol %) were mixed with 1.9 mM LUVs and samples were allowed to equilibrate for 15 min at 30°C before the measurements. The buffers were 20 mM Mops at pH 7.5 or pH 4.0. All measurements were taken in 3 mm wide cuvettes (sample volume = 150  $\mu$ L). Fluorescence polarization was measured on a PTI fluorimeter equipped with a Peltier device connected to a temperature controller. The widths of excitation and emission slits were 4 nm. The excitation and emission wavelengths were 350 nm and

420 nm, respectively. Measurements were started at 10°C and the temperature was increased gradually to 40°C with steps of 2°C. An equilibration time of 2 min was allowed after each temperature change. For each temperature, the emission fluorescence was recorded for 1 min and averaged. The vertically and horizontally polarized emission intensities were corrected for background scattering by subtraction of the corresponding polarized intensities of a blank containing an unlabeled LUV suspension. Steady-state fluorescence anisotropy was determined according to the following equation (16):

$$r = \frac{I_{VV} - GI_{VH}}{I_{VV} + 2GI_{VH}}, \quad (1)$$

where  $I_{VV}$  and  $I_{VH}$  are the emission intensities measured with the excitation polarizer set in the vertical direction and the emission polarizer oriented in the vertically or horizontally direction, respectively. The instrumental factor  $G$  ( $G = I_{HV}/I_{HH}$ ) was determined by measuring the emission intensities of the fluorescent probe with the excitation polarizer oriented in the horizontally direction.

### FRET measurements

Measurements were carried out using a SLM-Aminco 8000C spectrofluorimeter (ISS, Champaign, IL) equipped with a thermo-bath RTE-111 (Neslab). The widths of the excitation and emission slits were 4 nm. Energy transfer between aromatic residues of pHLIP excited at 280 nm and TMA-DPH (0.2 mol %) incorporated in DMPC or POPC bilayers was recorded over the wavelength range from 290 to 540 nm as a function of temperature. Measurements were started at 35°C and the temperature was lowered to 15°C in steps of 5°C. The molar ratio of pHLIP to lipids was 0.25 mol % and the concentration of lipids was 0.85 mM. The buffers used in the experiments were 20 mM Mops at pH 7.5 or pH 4.3. Light scattering and fluorescence backgrounds of a blank containing TMA-DPH inserted into LUVs were subtracted from the spectra.

### CD spectroscopy

Measurements were carried out using a CD spectrometer model 215 (Aviv, Lakewood, NJ). All spectra were recorded over the wavelength range from 200 to 280 nm with a 1 nm wavelength step and 3.0 s averaging time. Samples were measured in a 1.0 cm path length cuvette, with a sample volume of 3 mL, at 37°C. Peptide concentrations were checked at the end of each assay by quantitative amino acid analysis and these values were used to normalize the mean residue ellipticity. Two scans were averaged for each sample and the appropriate background contribution, i.e., buffer with or without LUVs, was subtracted from the spectra.

### Calcein leakage experiments

The dried POPC lipid film was rehydrated with 50 mM calcein in 10 mM Mops, 150 mM NaCl, 5 mM EDTA, pH 7.4. LUVs were prepared using the standard procedure and the free dye was removed by passage over a HiPrep 26/10 Desalting column (Sephadex G-25 Fine) pre-equilibrated with the same buffer. The total lipid concentration was adjusted with buffer to a final concentration of 0.1 mM. The LUV sample was kept at 4°C for a maximum of 3 days. Calcein leakage from the vesicles was monitored by measuring the decrease of self-quenching (excitation and emission wavelengths were set at 450 nm and 515 nm, respectively). The widths of excitation and emission slits were 2 nm. The percentage of dye released from the vesicles was calculated using the equation (17):

$$\%release = 100 \times (I_F - I_B)/(I_T - I_B), \quad (2)$$

where  $I_B$  is the background (self-quenched) intensity of calcein encapsulated in vesicles,  $I_F$  is the enhanced fluorescence intensity resulting from the

dilution of dye in the medium,  $I_T$  is the total fluorescence intensity after complete permeabilization by addition of 0.05% Triton X-100 from a 20% stock solution.

### Quenching of pHLIP intrinsic fluorescence by acrylamide

Experiments were carried out by measuring the fluorescence intensity of pHLIP in separate samples containing increasing concentrations of acrylamide taken from a 2 M stock solution. Measurements were taken at pH 7.5 or pH 4.5 in the presence of DMPC LUVs at 35°C and 15°C, or in the presence of DPPC LUVs at 35°C. The excitation wavelength was 280 nm and emission spectra were recorded between 290 and 420 nm. The inner filter effect was corrected using the following equation (16):

$$F_{\text{corr}} = F_{\text{obs}} \times 10^{(A_{\text{ex}} + A_{\text{em}})/2}, \quad (3)$$

where  $F_{\text{corr}}$  and  $F_{\text{obs}}$  are the corrected and observed fluorescence intensities, respectively.  $A_{\text{ex}}$  and  $A_{\text{em}}$  are the measured absorbance at the excitation and emission wavelengths, respectively. Quenching data were analyzed by a fit to the Stern-Volmer equation (16):

$$F_0/F = 1 + K_{\text{SV}}[Q], \quad (4)$$

where  $F_0$  and  $F$  are the fluorescence intensities in the absence and in the presence of the quencher, respectively,  $[Q]$  is the molar quencher concentration (in M) and  $K_{\text{SV}}$  is the Stern-Volmer quenching constant (in  $\text{M}^{-1}$ ).

### Depth measurements by bromine quenching of pHLIP intrinsic fluorescence

Collisional quenching of tryptophan fluorescence by brominated phospholipids ( $\text{Br}_2$ -PCs) was used to assess the depth of insertion of these residues in the lipid bilayer.  $\text{Br}_2$ -PCs are considered to be appropriate for this purpose because they are thought to minimally perturb the membrane. Bromine quenching of pHLIP was analyzed as a function of temperature. After mixing 0.25 mol % pHLIP with 0.6 mM DMPC LUVs with or without 30 mol % (6,7) $\text{Br}_2$ -PC incorporated in the bilayer, fluorescence emission spectra were recorded on excitation at 280 nm, at pH 7.5 or pH 4.5, and at temperatures above (35°C) and below (15°C)  $T_m$ . The difference of pHLIP quenching between the two conditions indicates a difference in depth of penetration of pHLIP adsorbed at the bilayer surface. Accordingly, the depth of the tryptophan residues was calculated by the parallax method using an additional sample of 0.25 mol % pHLIP mixed with 0.6 mM DMPC LUVs containing 30 mol % (9,10) $\text{Br}_2$ -PC. The differences in quenching of pHLIP fluorescence by (6,7)- and (9,10) $\text{Br}_2$ -PC incorporated separately in DMPC LUVs allow the calculation of the probability for the localization of tryptophan residues in the bilayer using the following equation (18):

$$z_{\text{cF}} = L_{\text{c1}} + \{[(-1/\pi C)\ln(F_1/F_2) - L_{21}^2]/2L_{21}\}, \quad (5)$$

where  $z_{\text{cF}}$  is the depth of the fluorophore as measured from the center of the bilayer,  $L_{\text{c1}}$  is the distance of the center of the bilayer from the shallow quencher,  $L_{21}$  is the difference in depth between the two quenchers,  $F_1$  is the fluorescence intensity in the presence of the shallow quencher,  $F_2$  is the fluorescence intensity in the presence of the deep quencher, and  $C$  is the two-dimensional quencher concentration in the plane of the membrane (molecules/ $\text{\AA}^2$ ).

## RESULTS

### Membrane permeability

Our previous data indicated that pHLIP induces membrane distortion of human RBCs at neutral pH, but no leakage of hemoglobin was observed (4), nor was there disruption of

vesicles encapsulating ANTS or DPX (3). To confirm that pHLIP does not induce gross membrane leakage over a wide range of peptide concentrations, the inability of pHLIP to cause the release of entrapped vesicle contents was checked at room temperature by monitoring the fluorescence intensity of calcein encapsulated in POPC liposomes at high self-quenching concentrations (Fig. 1). The appearance of fluorescence is a sensitive measure of vesicle permeability. As a positive control, the experiment was also carried out using a lytic peptide (melittin, from honey bee venom), which can form pores in cell membranes (19). The comparison between melittin and pHLIP confirms that membrane integrity is preserved at low concentrations of pHLIP.

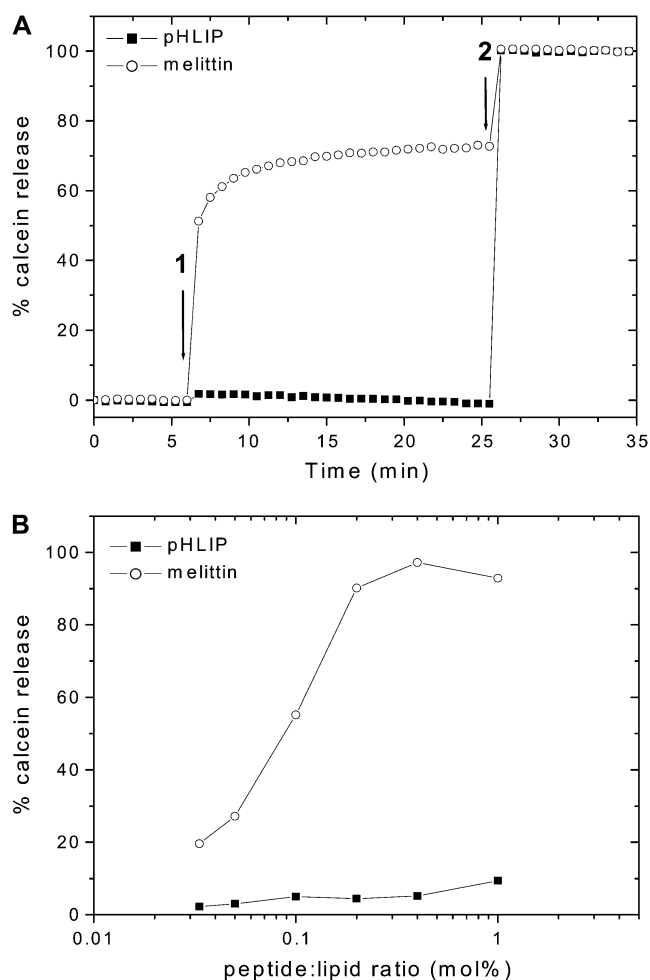


**FIGURE 1** Effect of pHLIP versus melittin on the membrane leakage. (A) Kinetics of calcein leakage. The release of calcein (50 mM) encapsulated in POPC vesicles was monitored by the increase in fluorescence intensity at 515 nm (excitation at 450 nm), on addition of 0.2 mol % melittin or pHLIP (arrow 1). Complete leakage was achieved on addition of 0.05% Triton X-100 (arrow 2). The percentage of calcein release was calculated as described in Materials and Methods. The total lipid concentration was 0.1 mM and the buffer was 10 mM Mops, 150 mM NaCl, 5 mM EDTA, at pH 7.4. (B) Calcein release versus peptide concentrations. The intensity was recorded after 30 min incubation in the dark at room temperature.

## Membrane fluidity

To study the effects of pHLIP on membrane fluidity, we measured changes in fluorescence anisotropy of a fluorescent probe (TMA-DPH) incorporated in DMPC bilayers versus temperature (Fig. 2). Fluorescence anisotropy reports the degree of rotational mobility of a fluorescent molecule and, therefore, it highly depends on the viscosity of the medium in which the fluorophore is dissolved. Anisotropy values can be used to probe the microviscosity of lipid membranes into which the fluorophore partitions (see (20) for review). TMA-DPH is a hydrophobic molecule, which is anchored at the water/lipid interface due to its charged trimethylammonium group. This fluorophore reports then on the mobility of the

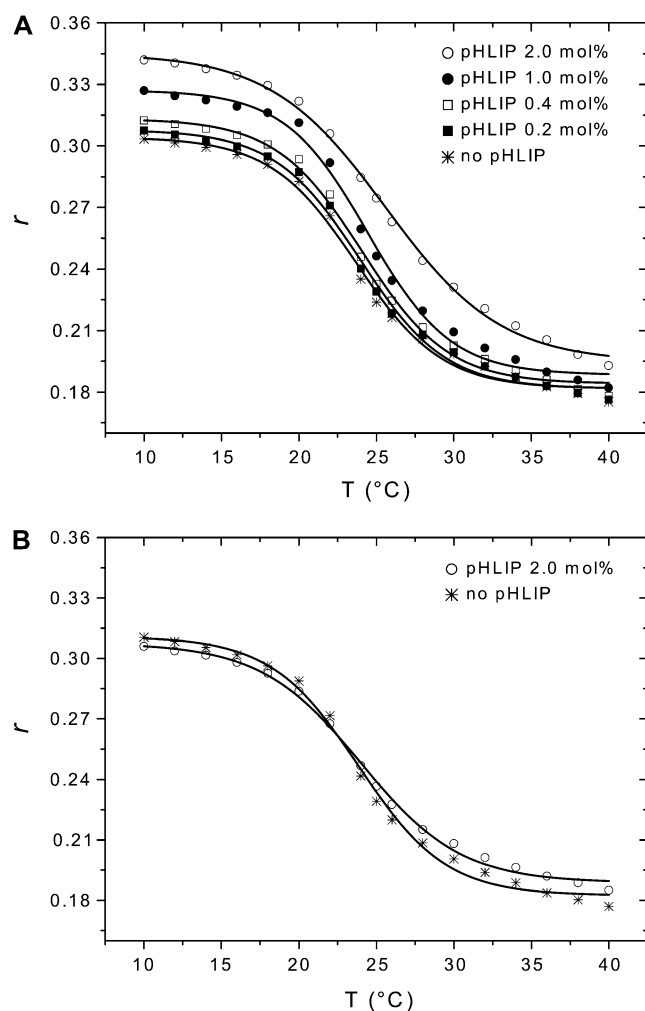


FIGURE 2 Effect of pHLIP on lipid membrane fluidity. The fluorescence anisotropy of TMA-DPH incorporated in DMPC bilayers was monitored in the presence of pHLIP at pH 7.5 (A) or pH 4.0 (B). Several concentrations of pHLIP (0.2, 0.4, 1.0, and 2.0 mol %) were tested with 1.9 mM DMPC LUVs containing 0.2 mol % TMA-DPH. The samples were excited by polarized light at 350 nm and emission was monitored at 420 nm. The fluorescence anisotropy was calculated as described in Materials and Methods and plotted as a function of temperature. Experimental points were fitted with a sigmoid function. The buffer was 20 mM Mops, at pH 7.5 or pH 4.0.

lipid headgroup region of membranes (21,22). Below  $T_m$  (23°C), DMPC lipids are in a gel phase, which is characterized by a low fluidity and slow lateral and rotational diffusions, whereas above this temperature, they are in the liquid-crystal state, which is characterized by a high fluidity and a fast diffusion (see (23) for review). Changes in anisotropy values of TMA-DPH from 0.18 to 0.31 with a decrease of temperature follow the phase transition of DMPC lipids. In the presence of low concentration of pHLIP at pH 7.5, there are no significant changes in the anisotropy. However, at high peptide concentration (2.0 mol % pHLIP or low lipid/peptide ratio of 50:1) the anisotropy values increase  $\sim 10\%$ , especially at low temperatures. This effect is a consequence of pHLIP interaction with the outer leaflet of bilayers, consistent with the induction of membrane perturbations, and it is enhanced by increasing peptide concentration. Interestingly, surface binding of pHLIP increases the value of  $T_m$  by  $\sim 2^\circ\text{C}$  for DMPC. The increase in anisotropy at low temperatures cannot be associated with better binding of pHLIP to the lipid bilayer, because thermodynamics data show clearly that the adsorption constant of pHLIP by POPC vesicles is 2 times lower at 15°C than at 35°C (5). At pH 4.0, i.e., when the peptide is inserted across the membrane, almost no difference is observed with regard to the membrane viscosity, even in the presence of 2.0 mol % pHLIP. Identical results were obtained with the fluorescent probe DPH, which reports on the order of hydrophobic chains in the core region of bilayers.

## Depth of penetration of pHLIP adsorbed at the bilayer surface

The penetration depth of surface-bound pHLIP into bilayers in the liquid-crystal and gel phases was estimated by analysis of quenching of pHLIP emission by brominated lipids ( $\text{Br}_2\text{-PCs}$ ) versus temperature. In Fig. 3, fluorescence spectra are reported for pHLIP, at pH 7.5 or 4.5, in the presence of DMPC LUVs with and without  $\text{Br}_2\text{-PCs}$ . Comparison of fluorescence quenching of membrane surface-bound pHLIP at 35°C and 15°C, i.e., at temperatures above and below  $T_m$  respectively (Fig. 3, A and B), shows a less significant quenching at high temperature than at low temperature. The quenching efficiency of pHLIP by  $\text{Br}_2\text{-PC}$  is  $\sim 10\%$  at 35°C and  $\sim 20\%$  at 15°C. At pH 4.5 (Fig. 3, C and D), the quenching efficiency is insignificantly affected by the phase transition ( $\sim 53\%$  at 35°C and  $\sim 54\%$  at 15°C). The position of maximum of pHLIP emission shifts toward long and short wavelengths as a result of quenching by  $\text{Br}_2\text{-PCs}$  at neutral and low pHs, respectively. Because tryptophan residues contribute much more to emission fluorescence than tyrosine and phenylalanine residues on excitation at 280 nm, we can attribute the fluorescence of pHLIP to tryptophan residues. Therefore, the observed shift suggests heterogeneity of tryptophan residue locations in the lipid bilayer in both states, which correlates well with our previous fluorescence decomposition analysis that showed two populations of tryp-

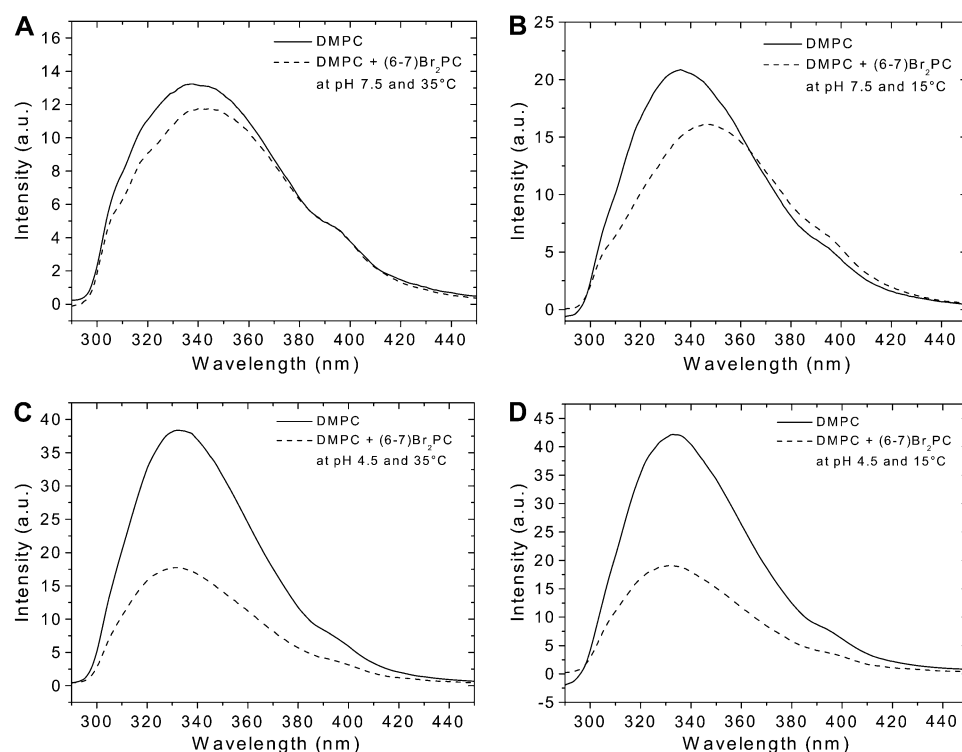


FIGURE 3 Quenched emission spectra of pHLIP by brominated lipids. pHLIP (0.25 mol %) was mixed with 0.6 mM unlabeled DMPC LUVs or DMPC LUVs containing 30 mol % (6,7) Br<sub>2</sub>-PC. Fluorescence emission spectra of pHLIP were recorded at 35°C (A and C) and 15°C (B and D). The buffer was 20 mM Mops, pH 7.5 (A and B) or pH 4.5 (C and D).

tophan residues with emission at 326 and 347 nm in the membrane-adsorbed state, and 321 and 339 nm in the inserted state (3). In the case of the absorbed peptide, bromine atoms more efficiently quench the emission of the buried tryptophan residue (which emits with a maximum at 326 nm), leading to the significant long-wavelength shift of fluorescence ( $\sim 2$  nm at 35°C and  $\sim 8$  nm at 15°C). However, at low pH, when the peptide is inserted, the presence of Br<sub>2</sub>-PCs induces a slight short-wavelength shift in emission ( $\sim 1$  nm at both temperatures) and enhanced quenching, which might suggest an interaction of both tryptophan residues with bromine atoms (with some predominance in the interaction of the tryptophan residue that emits with a maximum at 339 nm). The enhanced wavelength shift and quenching efficiency of pHLIP adsorbed to a DMPC bilayer surface in the gel phase in comparison with the liquid phase might suggest deeper burial of tryptophan residue in the core of the bilayer.

Applying the parallax method (18), the penetration depth of tryptophan residues of pHLIP adsorbed to the bilayer surface was calculated from the magnitude of quenching measured for vesicles containing either (6,7)- or (9,10)Br<sub>2</sub>-PCs. Because there is a clear heterogeneity of tryptophan location in the lipid bilayer, the values obtained from the parallax method are likely to be associated with the tryptophan residues located close to bromine atoms. An important value needed for the calculation of depth is the distance of each quencher from the bilayer center. Using x-ray diffraction, these distances have been determined for a series of Br<sub>2</sub>-PCs structured in POPC bilayer-like in the liquid-crystal

phase (24,25), but they need to be known in DMPC bilayers in both phases, because the bilayer thickness changes with acyl chain length (26) and with the phase transition. In the last case, the thickness variations are due to a rigidification of fatty acyl chains and concern mainly the hydrophobic core (27). The thickness of DMPC bilayers in the crystal-liquid phase has been determined to be 35.3 Å for the head-head thickness, i.e., the distance between the phosphate groups, and 25.4 Å for the hydrocarbon core region (28). In the gel phase, the thickness has been determined to be 40.1 Å for the head-head spacing and 30.3 Å for the hydrophobic core region (29). Based on these values and assuming a uniform hydrocarbon chain packing across the bilayer, the increments per CH<sub>2</sub> group are equal to 0.907 Å/CH<sub>2</sub> and 1.08 Å/CH<sub>2</sub> in the liquid-crystal and gel phases, respectively. By using the same assumptions reported by McIntosh and Holloway (24), we can make a rough calculation of the distance of each quencher from the bilayer center. We assume the following: i), the averaged quencher distances from the bilayer center are at the averaged positions of the carbon atoms of the fatty acyl chain to which the bromine atoms are attached; and ii), the distance between apposing terminal methyl groups is twice the separation of adjacent methylenes, because the volume of CH<sub>3</sub> is about twice the volume of a CH<sub>2</sub> group (30,31). Consequently, an extra CH<sub>2</sub> increment that corresponds to the distance between the terminal methyl group and the bilayer center is added in the acyl chain length. The respective distances of quenchers from the bilayer center were, therefore, estimated to be 7.7 Å and 9.2 Å for (6,7)Br<sub>2</sub>-PC in

the liquid-crystal and gel phases, respectively. For (9,10)Br<sub>2</sub>-PC, these distances are 5.0 Å and 5.9 Å in the liquid-crystal and gel phases, respectively. The depth values  $z_{\text{CF}}$  of one of tryptophan residues of pHLIP adsorbed at the membrane surface were, then, calculated to be  $8.0 \pm 0.1$  Å at 35°C and  $7.6 \pm 0.2$  Å at 15°C from the center of the bilayer. These distances correspond to distances of 9.7 Å at 35°C and 12.5 Å at 15°C from the positions of phosphate groups in the membrane.

Measurements of quenching of pHLIP emission by acrylamide also were done. Here, we examine changes of the acrylamide quenching rate of tryptophan emission from pHLIP mixed with DMPC or DPPC LUVs at low and high temperatures and pH values. The slope of the Stern-Volmer plot gives the Stern-Volmer constant ( $K_{\text{SV}}$ ). This parameter provides information about the accessibility of tryptophan residues to the quencher. Acrylamide quenching experiments were done at pH 7.5 and pH 4.5 with DMPC LUVs at either 35°C (liquid-crystal phase) or 15°C (gel phase), and with DPPC LUVs at 35°C (gel phase). The averaged Stern-Volmer constants are reported in Table 1. The value of  $K_{\text{SV}}$  obtained at pH 7.5 and in the absence of bilayers, i.e., when the peptide is present in solution, is close to that expected for completely water-accessible tryptophan ( $K_{\text{SV}} = 16 \text{ M}^{-1}$ ) (16). This result supports the idea that the peptide is well exposed to the solution and does not form clusters. In the presence of DMPC bilayers in the liquid-crystal phase (at 35°C), the  $K_{\text{SV}}$  value is lower due to the peptide binding to a bilayer and burial of tryptophan residues into it. The value of  $K_{\text{SV}}$  ( $6.8 \text{ M}^{-1}$ ), which is the average value for both tryptophan residues (buried and exposed) is 46% of the relative  $K_{\text{SV}}$  value calculated for the completely exposed tryptophan residues (100%). This value correlates well with the averaged value of  $K_{\text{SV}}$  (48%) obtained from the decomposition analysis (3). When the pH is titrated to pH 4.5, the  $K_{\text{SV}}$  constant found is close to the value expected for completely shielded tryptophan ( $K_{\text{SV}} = 1.2 \text{ M}^{-1}$ ) (32), because the insertion of pHLIP in membranes results in burial of both tryptophan residues. This value correlates well with the averaged value of the relative  $K_{\text{SV}}$  constant (15%) obtained as a result of decomposition analysis. At 15°C, the DMPC bilayer is in the gel phase state and the measured  $K_{\text{SV}}$  constant is lower for pH 7.5 (29%) compared to the respective value obtained at 35°C,

which is an additional evidence that a part of pHLIP is buried more deeply in the lipid bilayer in the gel phase. To test whether the temperature and the phase have an effect on quenching efficiency, this experiment was carried out at 35°C in DPPC bilayers, which are in a gel phase state ( $T_{\text{m}} = 41.5^\circ\text{C}$ ) (33). The value of  $K_{\text{SV}}$  determined at pH 7.5 is close to that obtained in DMPC at 15°C, confirming the absence of temperature effect on quenching efficiency and proving the influence of the lipid phase on quenching of pHLIP fluorescence. At pH 4.5, the value of  $K_{\text{SV}}$  is close to that obtained in DMPC at 35°C, suggesting the absence of any measurable phase effect on quenching efficiency.

### Insertion assay

The overlap between the emission spectrum of tryptophan residues and the excitation spectrum of TMA-DPH enables FRET from one to the other. This pair of fluorophores was already used in previous studies and the  $R_0$  distance, i.e., the distance at which 50% of energy transfer is efficient, was determined to be between 34–39 Å (34,35), so we took advantage of the opportunity to make FRET measurements to explore pHLIP binding and insertion in lipid bilayers. Fig. 4, A and B, show emission fluorescence spectra of pHLIP at pH 7.5 and pH 4.3 in the presence of pure POPC bilayers or POPC bilayers containing TMA-DPH, respectively. When pHLIP is inserted into the lipid bilayer as a transmembrane helix, a FRET signal is observed, whereas at neutral pH, when the peptide is adsorbed on the membrane surface, there is no significant energy transfer. Even at low pH the energy transfer is not very efficient considering that  $R_0$  is  $\sim 40$  Å. In a related study, no energy transfer was observed for melittin interacting with a lipid bilayer containing TMA-DPH at low lipid/peptide molar ratio of 60:1 (35). The authors carried out a very careful analysis of the probability of contacts between a randomly distributed dye in the bilayer and melittin, and concluded that the average distance between peptide and dye is more than 40 Å. The enhanced efficiency of energy transfer in case of pHLIP inserted into lipid bilayers indicates closer contact between one of the tryptophan residues and TMA-DPH. Our interpretation is that, in the membrane-adsorbed state of pHLIP, one tryptophan residue is located outside the membrane (347 nm) and the other is buried in the lipid bilayer (326 nm), and that they are both too far from TMA-DPH to produce any significant energy transfer. In the inserted form of pHLIP, one tryptophan residue (the exposed one with emission at 339 nm) is most likely to be located at level of headgroups and in close contact with TMA-DPH, which enhances the energy transfer. Further, our view is supported by the observation of a slight short-wavelength shift of pHLIP emission after FRET (see Figs. 4 B or 6 A). Also, the total quantum yield of tryptophan residues (quantum yield of donor) buried inside lipid bilayers is enhanced and the  $R_0$  value, which depends on donor quantum yield, is expected to increase.

**TABLE 1** Stern-Volmer quenching constant  $K_{\text{SV}}$  of acrylamide for pHLIP

|        | $K_{\text{SV}} (\text{M}^{-1})$ |         |      |                 |
|--------|---------------------------------|---------|------|-----------------|
|        | In buffer<br>35°C               | In DMPC |      | In DPPC<br>35°C |
|        |                                 | 35°C    | 15°C |                 |
| pH 7.5 | 14.8                            | 6.8     | 4.3  | 4.0             |
| pH 4.5 | —                               | 2.3     | —    | 2.1             |

pHLIP (0.25 mol %) was mixed with 0.6 mM DMPC LUVs or DPPC LUVs. The buffer was 20 mM Mops, pH 7.5 or pH 4.5.

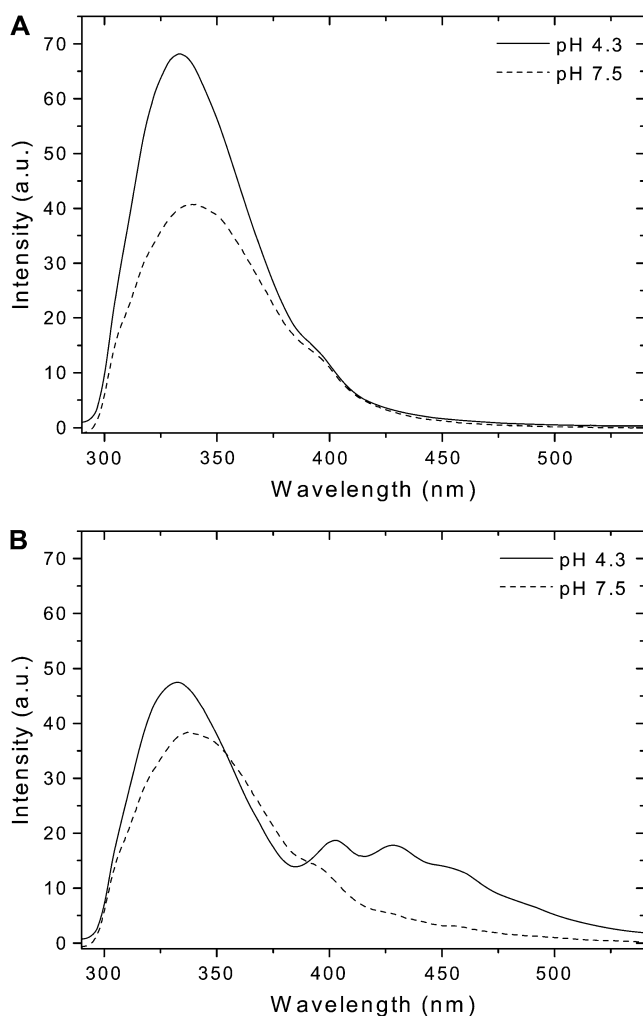


FIGURE 4 pH-dependence of FRET process between pHLIP and TMA-DPH incorporated in the membrane. pHLIP (0.33 mol %) was mixed with 0.85 mM POPC LUVs (A) or POPC LUVs containing 0.2 mol % TMA-DPH (B). The samples were excited at 280 nm at 20°C. The buffer was 20 mM Mops, at pH 7.5 or pH 4.3. Light scattering and fluorescence backgrounds of a blank containing TMA-DPH inserted into LUVs were subtracted from the spectra.

Additional evidence of bilayer perturbations accompanied by a deeper position of pHLIP adsorbed to the bilayer surface is given by the changes in the FRET signal with temperature. For this purpose, pHLIP was mixed with either POPC or DMPC bilayers containing TMA-DPH at pH 4.3 or pH 7.5 and emission fluorescence spectra were monitored versus temperature. These two lipid types were chosen because in the temperature range tested (15°C–35°C) POPC bilayers are in the liquid-crystal phase, whereas DMPC bilayers have a gel-to-liquid crystal phase transition at 23°C. To correct for the temperature effects on fluorescence intensities, the ratios of emission intensities recorded at 333 and 430 nm at pH 4.3 or recorded at 340 and 430 nm at pH 7.5 are shown in Fig. 5 rather than the absolute intensities. In the presence of POPC bilayers at pH 4.3, the FRET signal increases linearly with

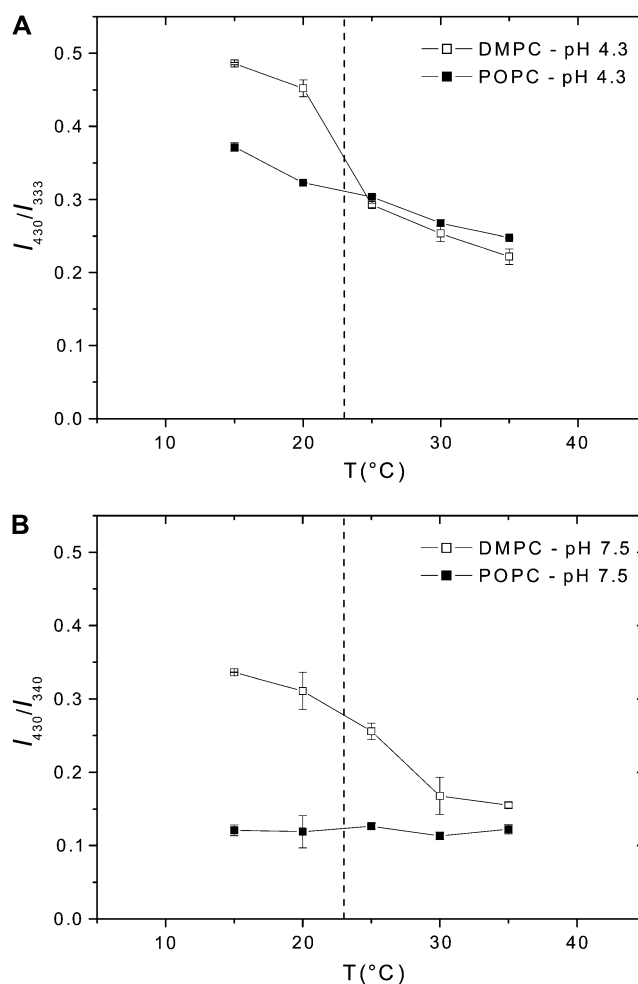


FIGURE 5 Temperature-dependence of pHLIP fluorescence in the presence of membranes. pHLIP (0.25 mol %) was mixed with either 0.85 mM POPC LUVs or DMPC LUVs at pH 4.3 (A) or pH 7.5 (B). Samples were excited at 280 nm and the emission fluorescence was observed as a function of temperature. Data are plotted as the ratio of intensities at 333 and 430 nm for samples at pH 4.3, and at 340 and 430 nm for samples at pH 7.5 to cancel out the effect of fluorescence quenching due to temperature variations. The dashed line indicates  $T_m$  of phase transition for DMPC at 23°C.

cooling temperature. The value of the FRET signal is ~30% stronger at 15°C than at 35°C probably because of changes in the degree of hydration of the bilayer. In the presence of DMPC, the signal is similar to that obtained in POPC at temperatures above  $T_m$ , but a jump is observed below  $T_m$ . At 15°C, the signal was ~23% higher in DMPC than in POPC and this difference is associated with rigidification of the DMPC bilayer due to the phase transition. On the other hand, in POPC at pH 7.5, the value of the FRET signal is insignificant (Fig. 3 B), so it stays low and stable over the temperature changes. In DMPC, the value of the FRET signal is close to that obtained in POPC at 35°C, whereas it is 53% higher at 15°C. A tentative of interpretation of this observation is a deeper position of a part of pHLIP in the gel phase compared to the fluid phase. No variation of the ellipticity

signal was observed by CD after the phase transition, which means that the variations in the binding mode do not significantly alter the secondary structure of the peptide.

### Peptide design

Our earlier biophysical studies and those presented here advance our understanding of the interactions of moderately polar peptides, like pHLIP, with a lipid bilayer. To broaden the case, we include the beginnings of an effort to find the key elements of the amino acid sequence that give pHLIP its properties. We first studied variants that differ from the wild-type peptide by the replacement of two aspartate residues present in the transmembrane domain by either asparagines (N-pHLIP) or lysines (K-pHLIP). Those peptides were tested for their ability to insert in membranes (4), and it was shown that the pH-dependent insertion was affected: N-pHLIP is present mainly in its helical form and inserts in membranes at both high and low pHs (but less efficiently than the wild-type peptide) whereas K-pHLIP is mainly unstructured. Both of them exhibit aggregation in aqueous solutions. An additional

question that remained unanswered is how the aspartate residues located outside the transmembrane domain affect the insertion process. We compared the characteristics of the wild-type pHLIP with a variant in which its C-terminus is neutralized by replacing three negatively charged residues (two aspartates and one glutamate) by three polar, but neutral, residues (two asparagines and one glutamine). The assay using FRET, described above, was used for testing the insertion ability of pHLIP and the variant, which were mixed separately with POPC bilayers containing TMA-DPH at pH 7.4 and pH 4.2 (Fig. 6, *A* and *B*). In contrast to the wild-type peptide, the FRET signal obtained for the variant is not enhanced after titrating pH 7.4 to 4.2 and no blue-shift is observed, showing modified efficiency of insertion of the variant. On the other hand, the CD spectra show that the secondary structure of pHLIP is strongly affected by the change of these residues in its C-terminus: at pH 7.8, with or without a lipid bilayer, the variant presents a mixture of helical and random structures, whereas the wild-type peptide is completely unstructured (Fig. 6, *C* and *D*). A drop of pH leads to an increase of helicity. Replacement of the negative residues

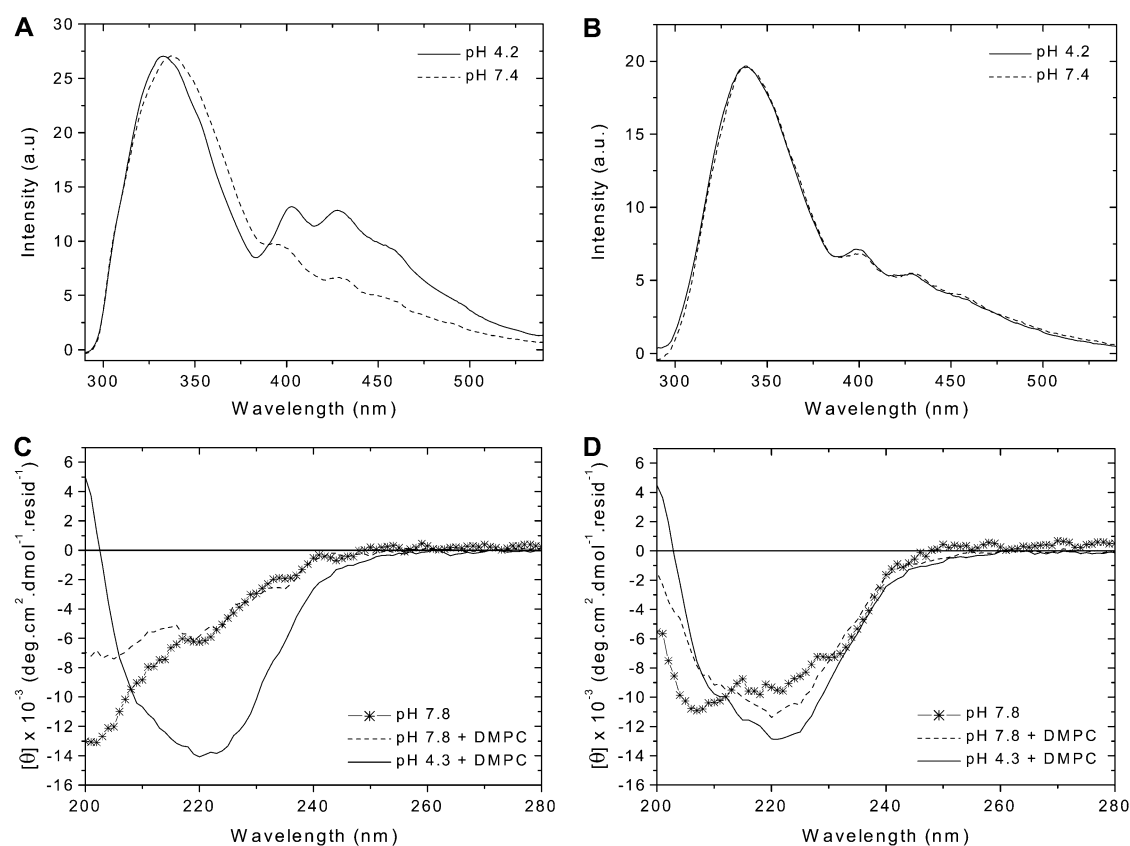


**FIGURE 6** Insertion ability and secondary structure of wild-type and variant pHLIP peptides. The peptides (0.2 mol %) were separately mixed with 0.85 mM POPC LUVs containing 0.2 mol % TMA-DPH at pH 7.4 or pH 4.2. The emission fluorescence spectra of wild-type (*A*) and variant (*B*) peptides, after excitation at 280 nm, were corrected for light scattering and fluorescence background, and were normalized to the maximal intensity. The buffer was 20 mM Mops. The peptides (0.8 mol %) were analyzed by CD spectroscopy without or with 0.37 mM DMPC LUVs at 37°C, at pH 7.8 and pH 4.3. The CD spectra of wild-type (*C*) and variant (*D*) peptides were corrected for the background contribution, and were smoothed in a window of three points. The buffer was 2 mM Tris-HCl, 5 mM NaCl.



by neutral ones changes the hydrophobic character of the peptide (using the octanol/water scale,  $\Delta G$  varies from 8.38 to  $-0.06$  kcal.mol $^{-1}$  (36)), which might lead to an aggregation of the peptide in solution and a reduction of its ability to insert into a lipid bilayer.

## DISCUSSION

In this study, we have examined biophysical properties of the interaction of pHLIP with lipid bilayers. Such properties are relevant both for improving our understanding of the insertion of peptides into membranes and for the development of therapeutic applications. Before insert, the first required step is the binding of the peptide to the surface of membranes, which is the focus of our analysis here. This study was motivated by previous data showing that pHLIP induces macroscopic perturbations of intact human RBCs (4). Accordingly, we investigated the pHLIP binding mode with the aim of gaining quantitative insights into the bilayer perturbations and interactions. All the results reported in this work were obtained on LUVs, a system used widely as a model for measurements of protein binding to and insertion into membranes.

From a pharmaceutical or toxicological point of view, any mechanism of cargo translocation resulting in gross permeabilization of the membrane would be unacceptable. The calcein leakage experiments were, therefore, carried out to check whether the peptide causes damage to pure phospholipid bilayers and to ensure that the binding of pHLIP does not lead to membrane permeabilization. The absence of calcein release from POPC vesicles in the presence of pHLIP at physiological pH (pH 7.4) confirms the absence of pore formation compared to melittin. This result is in agreement with earlier work (3,4). At neutral pH, the interactions of pHLIP with the biological membranes of human RBCs induce no leakage of hemoglobin while leading to the appearance of spicules on the surface of the majority of cells. The formation of spikes when the peptide is bound to the membrane is interpreted as the consequence of extra area occupied by pHLIP on the outer leaflet of the lipid bilayer. At pH 6, i.e., when the peptide is inserted into the membrane, a greatly reduced number of spikes is seen, which is consistent with pHLIP insertion across both halves of the bilayer. A related observation is obtained from lipid fluidity measurements using fluorescence anisotropy of TMA-DPH incorporated into the DMPC bilayer. Taking the lipid headgroup area as  $60.6 \text{ \AA}^2$  in the liquid-crystal phase (29) and the vesicle shape as a sphere of 100 nm diameter, the highest peptide concentration tested (2.0 mol %) corresponds to  $\sim 2000$  peptides per vesicle, or a low lipid/peptide ratio of 50:1. Under these conditions, the pHLIP association with the bilayer surface gives rise to an increase of lipid microviscosity and a rise in the  $T_m$  of the DMPC phase transition, whereas no significant perturbation occurs when pHLIP is adsorbed on the membrane surface at lower concentration or inserted

across the bilayer. Our data are in good agreement with our isothermal titration calorimetry results, which show two types of pHLIP interactions with lipid bilayers at low and high lipid/peptide ratios (5). We found that in the membrane-bound state at low and high lipid/peptide ratios pHLIP interacts with  $\sim 60$  and  $\sim 120$  lipids and that an additional 50–60 and 80–100 lipids are affected (destabilized), respectively, whereas the inserted peptide interacts with only  $\sim 22$  lipids, which is approximately the first surrounding layer for a transmembrane helix.

In earlier studies from the Huang laboratory, the interactions of a helical amphiphilic peptide (Alamethicin) with bilayers were analyzed in detail by x-ray lamellar diffraction (37). It was shown that the adsorbed peptides on the bilayer surface lead simultaneously to a disordering of the lipid chains and to a decrease of the bilayer thickness. The observed effects were ascribed to an increase of the cross sectional area in the polar region that requires accommodation by the lipids. Similarly, pHLIP increases the area of outer leaflet of membranes; however, it binds to the surface as an extended chain, rather than as a helix. Both pHLIP and amphiphilic helical peptides can be regarded as anisotropic inclusions into a leaflet of the bilayer, inducing membrane perturbations (38,39). However, the differences in conformation may lead to detailed differences in the interactions, perhaps including the extent of their insertion into the headgroups. An indication of this difference is seen in the deeper surface binding of pHLIP in the gel state and the increase of the transition temperature caused by pHLIP binding, indicating some stabilization of the gel state. This unexpected finding may be a worthy subject for further study.

Additional studies of pHLIP binding to the bilayer surface used fluorescence quenching experiments by either Br $_2$ -PCs or acrylamide. At pH 7.5, the acrylamide quenching Stern-Volmer constant and the fluorescence quenching efficiency by Br $_2$ -PCs change with the phase transition. In all cases, it appears that one tryptophan residue is more deeply buried in the bilayer than the other. This observation correlates well with our previous fluorescence decomposition analysis that showed two populations of tryptophan residues (3). The distance between the buried tryptophan residue of pHLIP and the center of the bilayer was evaluated by parallax analysis using (6,7)- and (9,10)Br $_2$ -PC as a pair of quenchers (18). The change of penetration depth after the phase transition was estimated to be  $0.4 \text{ \AA}$  from the bilayer center and  $2.8 \text{ \AA}$  from the bilayer phosphate groups given the bilayer thickness variation. Equilibrium of pHLIP intermediates adsorbed on the membrane surface could explain the differences observed in the gel and liquid-crystal phases. The propensity of the peptide to spontaneously insert into membranes, due to the presence of its hydrophobic residues, is thermodynamically opposed by the presence of its charged carboxylates. In this context, it may be useful to consider that the peptide binding to the bilayer is highly dynamic. This issue could be investigated by solution NMR spectroscopy, which can give dy-

namic information on the conformation of the peptide depending to the timescale of the intermediate equilibrium (40). Additional results at pH 4.5 indicate that, when the peptide is inserted across the bilayer, it does not induce significant perturbation and that variations due to the gel-to-liquid crystal phase transition are negligible.

We found that energy transfer from the aromatic residues of pHLIP to the fluorescent probe TMA-DPH anchored in the polar region of bilayers correlates with the surface binding and insertion of pHLIP. When the peptide is bound at the membrane surface (pH 7.5) no significant energy transfer is observed, whereas when pHLIP is inserted across the bilayer (pH 4.3) energy transfer is enhanced. The enhancement is associated most likely with closer contact between one of the tryptophan residues of pHLIP and TMA-DPH. The FRET assay done on various lipids at different pHs and temperatures further supported the results of bilayer perturbation at neutral pH, accompanied by a deeper position of pHLIP on the bilayer in the gel phase compared to the fluid phase.

The FRET assay was also used to compare pHLIP with a variant in which the charged Asp and Glu residues located on the C-terminus of the peptide were changed to the polar but uncharged side chains Asn and Gln, with the idea that the peptide insertion might be facilitated if the more polar groups did not have to be translocated. We observed the formation of elements of secondary structure for the variant in aqueous solution and suspect some form of self-association. Based on the FRET analysis, no significant insertion was seen even if we noticed by CD a shift toward helix formation at low pH in the presence of bilayers. Thus, this variation of the amino acid sequence may not prove useful, except as a caution that the combination of properties shown by pHLIP may be more difficult to create than we thought.

The design of sequences with controlled insertion properties should be aided by knowledge of peptide interactions with a bilayer. It is important that such a peptide preserves its ability to be monomeric in aqueous solution as well as when it is bound to the surface of a bilayer or inserted across it. This study advances our understanding of pHLIP interaction with cell membranes and strengthens the view that the mechanism of pHLIP interaction is different from the mechanism of amphipathic peptide interaction with a lipid bilayer, where the insertion involves cooperative oligomerization resulting in pore formation. The relaxation of lipid distortion has been proposed as a contributor to the insertion of amphipathic helices (37,41), but it is important to note that the case of pHLIP insertion differs in several respects. To consider the driving forces, one must examine the initial and final equilibrium states. Amphipathic helices bind at the bilayer surface and distort the lipid as folded helices and attain an inserted state that has both helix-helix contacts and helix-lipid contacts, because oligomers form during the process. On the other hand, pHLIP binds to the surface in an extended, unfolded form that distorts the lipid, but it is not established that the distortions are the same as those involved when the

different geometry of a helix is at the surface. The inserted pHLIP is a single helix, interacting only with lipid, so there is no need to separate the energies arising from helix-helix interactions from those arising from helix-lipid interactions. Thus, both the initial and final states of the two systems, amphipathic helices and pHLIP, differ. The distortion of lipids induced by pHLIP adsorption is not sufficient to induce peptide insertion, because pHLIP does not insert as a transmembrane helix with an increase of peptide concentration. Rather, the insertion mechanism of pHLIP is triggered by the increase of peptide hydrophobicity resulting from the protonation of negatively charged residues at low pH, which shifts the equilibrium toward partitioning of the peptide into the hydrophobic bilayer and the formation of a transmembrane helix. At the same time, because the interaction of pHLIP with the bilayer surface, which is the first step in the insertion process, distorts the lipids, and because the insertion across the bilayer relaxes the distortion, we conclude that the distortion energy of the bilayer might also contribute to the insertion.

We acknowledge Drs. Takemasa Kawashima and Oleg Andreev for discussion and comments on the manuscript. This work was supported by National Institutes of Health grants GM070895 and GM073857 to D.M.E.

## REFERENCES

- Hunt, J. F., P. Rath, K. J. Rothschild, and D. M. Engelman. 1997. Spontaneous, pH-dependent membrane insertion of a transbilayer  $\alpha$ -helix. *Biochemistry*. 36:15177–15192.
- Reshetnyak, Y. K., O. A. Andreev, U. Lehnert, and D. M. Engelman. 2006. Translocation of molecules into cells by pH-dependent insertion of a transmembrane helix. *Proc. Natl. Acad. Sci. USA*. 103:6460–6465.
- Reshetnyak, Y. K., M. Segala, O. A. Andreev, and D. M. Engelman. 2007. A monomeric membrane peptide that lives in three worlds: in solution, attached to, and inserted across lipid bilayers. *Biophys. J.* 93:2363–2372.
- Andreev, O. A., A. D. Dupuy, M. Segala, S. Sandugu, D. A. Serra, C. O. Chichester, D. M. Engelman, and Y. K. Reshetnyak. 2007. Mechanism and uses of a membrane peptide that targets tumors and other acidic tissues in vivo. *Proc. Natl. Acad. Sci. USA*. 104:7893–7898.
- Reshetnyak, Y. K., O. A. Andreev, M. Segala, V. S. Markin, and D. M. Engelman. Energetics of peptide (pHLIP) binding to and folding across a lipid bilayer membrane. PNAS, submitted.
- Wimley, W. C., and S. H. White. 2000. Designing transmembrane  $\alpha$ -helices that insert spontaneously. *Biochemistry*. 39:4432–4442.
- Killian, J. A. 2003. Synthetic peptides as models for intrinsic membrane proteins. *FEBS Lett.* 555:134–138.
- Ladokhin, A. S., and S. H. White. 2004. Interfacial folding and membrane insertion of a designed helical peptide. *Biochemistry*. 43:5782–5791.
- Popot, J. L., and D. M. Engelman. 1990. Membrane protein folding and oligomerization: the two-stage model. *Biochemistry*. 29:4031–4037.
- Popot, J. L., and D. M. Engelman. 2000. Helical membrane protein folding, stability, and evolution. *Annu. Rev. Biochem.* 69:881–922.
- Engelman, D. M., Y. Chen, C. N. Chin, A. R. Curran, A. M. Dixon, A. D. Dupuy, A. S. Lee, U. Lehnert, E. E. Matthews, Y. K. Reshetnyak, A. Senes, and J. L. Popot. 2003. Membrane protein folding: beyond the two stage model. *FEBS Lett.* 555:122–125.

12. White, S. H., and G. von Heijne. 2005. Transmembrane helices before, during, and after insertion. *Curr. Opin. Struct. Biol.* 15:378–386.
13. Ulmschneider, M. B., D. P. Tieleman, and M. S. P. Sansom. 2004. Interactions of a transmembrane helix and a membrane: comparative simulations of bacteriorhodopsin helix A. *J. Phys. Chem. B.* 108:10149–10159.
14. Vavere, A. L., O. A. Andreev, D. M. Engelman, Y. K. Reshetnyak, and J. S. Lewis. 2007. <sup>64</sup>Cu labeling and PET imaging of tumors in a small animal using a pH-dependent insertion of peptide <sup>64</sup>Cu-DOTA-pHLIP. *7th International Symposium on Radiopharmaceutical Sciences, Aachen, Germany.*
15. Stewart, J. C. 1980. Colorimetric determination of phospholipids with ammonium ferrothiocyanate. *Anal. Biochem.* 104:10–14.
16. Lakowicz, J. R. 1999. Principles of Fluorescence Spectroscopy. Kluwer Academic/Plenum, New York.
17. Benachir, T., and M. Lafleur. 1995. Study of vesicle leakage induced by melittin. *Biochim. Biophys. Acta.* 1235:452–460.
18. Chattopadhyay, A., and E. London. 1987. Parallax method for direct measurement of membrane penetration depth utilizing fluorescence quenching by spin-labeled phospholipids. *Biochemistry.* 26:39–45.
19. Matsuzaki, K., S. Yoneyama, and K. Miyajima. 1997. Pore formation and translocation of melittin. *Biophys. J.* 73:831–838.
20. Borenstain, V., and Y. Barenholz. 1993. Characterization of liposomes and other lipid assemblies by multiprobe fluorescence polarization. *Chem. Phys. Lipids.* 64:117–127.
21. Prendergast, F. G., R. P. Haugland, and P. J. Callahan. 1981. 1-[4-(Trimethylamino)phenyl]-6-phenylhexa-1,3,5-triene: synthesis, fluorescence properties, and use as a fluorescence probe of lipid bilayers. *Biochemistry.* 20:7333–7338.
22. Lentz, B. R. 1989. Membrane fluidity as detected by diphenylhexatriene probes. *Chem. Phys. Lipids.* 50:171–190.
23. Nagle, J. F., and S. Tristram-Nagle. 2000. Lipid bilayer structure. *Curr. Opin. Struct. Biol.* 10:474–480.
24. McIntosh, T. J., and P. W. Holloway. 1987. Determination of the depth of bromine atoms in bilayers formed from bromolipid probes. *Biochemistry.* 26:1783–1788.
25. Wiener, M. C., and S. H. White. 1991. Transbilayer distribution of bromine in fluid bilayers containing a specifically brominated analogue of dioleoylphosphatidylcholine. *Biochemistry.* 30:6997–7008.
26. Lewis, B. A., and D. M. Engelman. 1983. Lipid bilayer thickness varies linearly with acyl chain-length in fluid phosphatidylcholine vesicles. *J. Mol. Biol.* 166:211–217.
27. Leekumjorn, S., and A. K. Sum. 2007. Molecular studies of the gel to liquid-crystalline phase transition for fully hydrated DPPC and DPPE bilayers. *Biochim. Biophys. Acta.* 1768:354–365.
28. Kucerka, N., Y. Liu, N. Chu, H. I. Petrache, S. Tristram-Nagle, and J. F. Nagle. 2005. Structure of fully hydrated fluid phase DMPC and DLPC lipid bilayers using X-ray scattering from oriented multilamellar arrays and from unilamellar vesicles. *Biophys. J.* 88:2626–2637.
29. Tristram-Nagle, S., Y. Liu, J. Legleiter, and J. F. Nagle. 2002. Structure of gel phase DMPC determined by X-ray diffraction. *Biophys. J.* 83:3324–3335.
30. Wiener, M. C., and S. H. White. 1992. Structure of a fluid dioleoyl-phosphatidylcholine bilayer determined by joint refinement of x-ray and neutron diffraction data. II. Distribution and packing of terminal methyl groups. *Biophys. J.* 61:428–433.
31. Wiener, M. C., R. M. Suter, and J. F. Nagle. 1989. Structure of the fully hydrated gel phase of dipalmitoylphosphatidylcholine. *Biophys. J.* 55:315–325.
32. van Heusden, H. E., B. de Kruijff, and E. Breukink. 2002. Lipid II induces a transmembrane orientation of the pore-forming peptide lantibiotic nisin. *Biochemistry.* 41:12171–12178.
33. Vandijk, P. W. M., B. Dekruijff, L. L. M. Vandeenen, J. Degier, and R. A. Demel. 1976. Preference of cholesterol for phosphatidylcholine in mixed phosphatidylcholine-phosphatidylethanolamine bilayers. *Biochim. Biophys. Acta.* 455:576–587.
34. Tiriveedhi, V., and P. Butko. 2007. A fluorescence spectroscopy study on the interactions of the TAT-PTD peptide with model lipid membranes. *Biochemistry.* 46:3888–3895.
35. Bradrick, T. D., A. Philippidis, and S. Georghiou. 1995. Stopped-flow fluorometric study of the interaction of melittin with phospholipid bilayers: importance of the physical state of the bilayer and the acyl chain length. *Biophys. J.* 69:1999–2010.
36. Wimley, W. C., T. P. Creamer, and S. H. White. 1996. Solvation energies of amino acid side chains and backbone in a family of host-guest pentapeptides. *Biochemistry.* 35:5109–5124.
37. Wu, Y., K. He, S. J. Ludtke, and H. W. Huang. 1995. X-ray diffraction study of lipid bilayer membranes interacting with amphiphilic helical peptides: diphytanoyl phosphatidylcholine with alamethicin at low concentrations. *Biophys. J.* 68:2361–2369.
38. Markin, V. S. 1981. Lateral organization of membranes and cell shapes. *Biophys. J.* 36:1–19.
39. Bohinc, K., D. Lombardo, V. Kraljiglic, M. Fosnaric, S. May, F. Pernus, H. Hagerstrand, and A. Iglic. 2006. Shape variation of bilayer membrane daughter vesicles induced by anisotropic membrane inclusions. *Cell. Mol. Biol. Lett.* 11:90–101.
40. Cavanagh, J., W. J. Fairbrother, A. G. Palmer III, and N. J. Skelton. 1996. Protein NMR Spectroscopy: Principles and Practice. Academic Press, San Diego.
41. He, K., S. J. Ludtke, W. T. Heller, and H. W. Huang. 1996. Mechanism of alamethicin insertion into lipid bilayers. *Biophys. J.* 71:2669–2679.